

UDC 621.9.048.6

THE EFFECT OF ROUGHNESS ON THE PHYSICOCHEMICAL PROPERTIES OF A36 STEEL: PHOSPHATE ADHESION STUDY

Youssef Najih, Mustapha Adar*, Majda Medkour, Jamaa Bengourram,
Mustapha Mabrouki

Industrial Engineering Laboratory, Sultan Moulay Slimane University, Faculty of Science and Technology, Beni Mellal, Morocco
Received 2 May 2023; accepted 20 September 2023; available online 25 October 2023

Abstract

This work discusses the effect of surface roughness and surface physicochemical properties on the initial adhesion of phosphate to steel. The steel samples used in this study are made from A36 low alloy steel. The phosphate was extracted from the BenGurir-Morocco area and is used in this work in the form of pellets that were compacted using different pressures. The steel surface is treated by two methods of surface pretreatment such as honing and horizontal milling. The influence of this pretreatment procedure on the surface morphology, roughness, surface energy and hydrophobicity are examined. By measuring the contact angle on the surfaces of the phosphate pellets and the substrates of low-alloy A36 steel, we were able to identify the physicochemical parameters by calculating the surface energy. In addition, the roughness of each steel sample was investigated using the roughness meter and the metallurgical microscope. The results obtained showed that the phosphate surface is subject to dispersing forces and has a hydrophilic character. For the surfaces of different A36 steel substrates, the effect of roughness was well examined, the minimum surface energy was obtained for both pretreatment (honing and horizontal milling) for a determined roughness. This result can be used for preparing surfaces with minimum surface energy in order to minimize fracture energy and therefore minimize the adhesion and clogging of the phosphate on steels.

Keywords: Phosphate; low-alloy A36 steel; clogging; adhesion; surface energy; wetting.

ВПЛИВ ШОРСТКОСТІ НА ФІЗИКО-ХІМІЧНІ ВЛАСТИВОСТІ СТАЛІ А36: ДОСЛІДЖЕННЯ АДГЕЗІЇ ФОСФАТІВ

Юсеф Наджіх, Мустафа Адар*, Маджда Медкур, Джамаа Бенгуррам,
Мустафа Мабрукі

Лабораторія промислового інжинірингу, Університет Султана Мула Слімана, факультет науки і технологій, Бені Меллал, Марокко

Анотація

У цій роботі обговорюється вплив шорсткості поверхні та фізико-хімічних властивостей поверхні на початкову адгезію фосфатів до сталі. Зразки сталі, використані в цьому дослідженні, виготовлені з низьколегованої сталі А36. Фосфат був видобутий в районі Бен-Гурір-Марокко і в цій роботі використовувався у вигляді гранул, спресованих під різними тисками. Сталеву поверхню обробляли двома методами попередньої обробки поверхні – хонінгуванням та горизонтальним фрезеруванням. Досліджено вплив цих процедур на морфологію поверхні, шорсткість, поверхневу енергію та гідрофобність. Вимірюючи кут контакту на поверхнях фосфатних гранул і підкладок з низьколегованої сталі А36, ми змогли визначити деякі фізико-хімічні параметри та розрахувавши поверхневу енергію. Крім того, шорсткість кожного сталевого зразка була досліджена за допомогою вимірювача шорсткості та металургійного мікроскопа. Отримані результати показали, що фосфатована поверхня піддається впливу дисперсійних сил і має гідрофільний характер. Для поверхонь різних підкладок зі сталі А36 добре досліджено вплив шорсткості, отримано мінімальну поверхневу енергію як для попередньої обробки (хонінгування та горизонтального фрезерування), так і для визначеної шорсткості. Цей результат може бути використаний для підготовки поверхонь з мінімальною поверхневою енергією для мінімізації енергії руйнування і, отже, мінімізації адгезії та засмічення фосфатами сталі.

Ключові слова: фосфат; низьколегована сталь А36; засмічення; адгезія; поверхнева енергія; змочування.

*Corresponding author: e-mail: adar.mustapha@gmail.com

© 2023 Oles Honchar Dnipro National University;

doi: 10.15421/jchemtech.v31i3.278149

Introduction

In Morocco, the mining sector occupies a very important place in its economic plan, representing 21 % of export revenues. Since the beginning of the 20th century, large sources of phosphates have been discovered containing three quarters of the known reserves on the planet. The exploitation of phosphates is a monopoly of the Moroccan State represented by the Cherifian Phosphate Office (OCP) created in 1920. from extraction to treatment. Phosphate is generally transported by high-capacity trucks. One of the areas of research was the reduction of phosphate losses during transportation, because phosphate adheres to the walls of the truck body, which causes major problems, and also the high cost related to the number of transportation cycles, which results to long delivery times. The remaining problem is related to the adhesion phenomena between the phosphate and the steels (which make up the truck). Their close nature is likely to favor phenomena of diffusion or molecular interactions involved in phosphate adhesion. This adhesion is harmful for transport operations, slowing down production rates and thus creating a loss of income for the manufacturer.

Adhesion is a phenomenon that corresponds to the interfacial forces that occur when two surfaces are brought into contact [1]. These forces can be valence efforts and/or result from anchoring actions. It is thus the set of physical or chemical interactions that take place at the interface of two phases [2]. The main mechanisms of adhesion have been the subject of several studies [3–12] throughout the last century and it has become apparent that adhesion is systematically the result of a series of mechanisms. Recently, Awaja et al. put forward 3 main mechanisms to explain adhesion between two materials: mechanical anchoring, intermolecular bond formation and adhesion thermodynamics [6].

In nature we find a variety of materials that have a rough surface. This parameter (roughness) can be observed at the microscopic scale mainly due to the fabrication and implementation processes. Much work [13–19] deals with the influence of the roughness of a material on its wetting properties, and it is accepted that roughness affects the wetting properties of a material that is initially wetting [13] and the non-wetting properties of a material that is initially not very wetting [15; 17]. Roughness is also the only way to access hydrophobic and hydrophilic surfaces [13; 14]. A large number of studies have been devoted to studying the effect of the

physicochemical properties of the surface on the adhesion between a material and steel, which induces the formation of relatively strong acid-base interactions [20].

To date, to the best of our knowledge, no studies have systematically examined the influence of steel surface properties on the initial adhesion of phosphate. Therefore, the aim of this work is to obtain a better fundamental understanding of the mechanisms and phenomena responsible for initial adhesion between phosphate and steels. Our objective is to control the surface properties of steel bearing the reference A36 for the non-adhesion of phosphate on its surface. For this reason, we would like to modify the physicochemical properties by changing the roughness and pretreatment of the steel surface. Since the control of the physical chemistry of the surface will be of first importance, it is crucial to control the main parameters affecting it (surface energy, roughness), which allows to obtain a surface with low wetting properties to minimize the interactions causing adhesion phenomena between phosphate and steel. Using the droplet technique of a goniometer, we carried out contact angle measurements in order to calculate the surface energy of the steels. The results showed that each treatment of the steel surfaces achieved a minimum surface energy. Therefore, we also proved that roughness has a direct influence on the physicochemical properties and consequently on the adhesion of phosphates on A36 steels used in this study.

Material and Method

Phosphate Pellets Preparation. The purpose of this section is to describe the preparation of phosphate pellets from the phosphate rocks obtained from the BenGurir extraction area of Morocco, which were used to characterize the phosphate surfaces. To eliminate the interstices in volume during compression, we prepared the pellets with a 20 % water content. Specifically, we used a MAGNUS-England hydraulic press to compress 9 g of phosphate under different pressures (90, 110, 150, 210, 250 and 310 bar) for 5 minutes. The pellets were then heated at a temperature of 60 °C for 2 hours to promote sintering. We chose this temperature because it is below the melting point of phosphate and allows the formation of solid pellets without decomposition.

Pretreatment of A36 steel substrates. The low-alloy A36 steels were chosen due to their high strength and toughness, which are attributed to

their composition of 0.18 % carbon, 0.2 % copper, and 0.8 % manganese. To investigate the effect of surface roughness on the coating adhesion, we prepared five A36 steel substrates by honing with varying durations to obtain different roughness parameters (0.05 μm , 0.2 μm , 0.4 μm , 0.8 μm , and 1.6 μm). Additionally, we used horizontal milling to modify the roughness by adjusting the parameters of the cut, such as the speed of rotation of the tool and the table of the milling machine, resulting in five more substrates with roughness parameters of 0.4 μm , 0.8 μm , 1.6 μm , 3.2 μm , and 6.3 μm . Note that the honing and milling treatments were performed on separate substrates to avoid any cross-contamination.

Contact angle measurement. The contact angle measurements were conducted using the DIGIDROP device from GBX France. Droplets with a volume of approximately 10 μL were dispensed onto the sample surface using a micro-dispenser and a syringe with a 0.5 mm outer diameter needle. The droplets were allowed to fall from a height of 10 mm to minimize the effects of gravity. The device included a camera, a backlight system, and a sample holder for precise alignment. Contact angle measurements were performed using standard liquids: water and formamide, which are polar, and methylene iodide, which is non-polar [21–23]. The measurements were taken on both steel substrates and phosphate pellets to calculate

$$(\cos \theta + 1)/2 = (\gamma_s^{LW} \gamma_L^{LW})^{1/2} / \gamma_L + (\gamma_s^+ \gamma_L^-)^{1/2} / \gamma_L + (\gamma_s^- \gamma_L^+)^{1/2} / \gamma_L \quad (4)$$

To obtain the surface energy of a solid from at least 3 different liquids is required [27; 28].

Free energy of interaction (Hydrophobicity)

The quantitative hydrophobicity of a material (i) is defined by the change in the free energy of

$$\Delta G_{iwi} = -2[(\gamma_i^{LW})^{1/2} - (\gamma_i^{LW})^{1/2}]^2 + 2[(\gamma_i^+ \gamma_i^-)^{1/2} + (\gamma_w^+ \gamma_w^-)^{1/2} - (\gamma_i^+ \gamma_w^-)^{1/2} - (\gamma_w^+ \gamma_i^-)^{1/2}] \quad (5)$$

A negative value of ΔG_{iwi} (attractive free energy of interaction between molecules) indicates that solid surfaces have less affinity for water than for each other, implying a hydrophobic character. Conversely, a positive of ΔG_{iwi} implies a hydrophilic character of the solid surface.

Result and discussion

Physicochemical characterization of phosphate pellets. After 2 hours at 180 °C heating and compacting under different pressures (90, 110, 150, 210, 250 and 310 bar), contact angle measurements of three probe liquids are made on the surface of the phosphate pellets. The probe liquids used are water, formamide and diiodomethane. The values of the contact angles of these liquids in contact with the phosphate pellet

the surface energy. The surface energy components of the liquids were obtained from [24].

Surface energy calculation. The surface energy of a solid is characterized by the thermodynamic equilibrium of the three interactions solid/liquid γ_{SL} , solid/vapor γ_{SV} and liquid/vapor γ_{LV} , as stated by Thomas Young [25]. This equilibrium is expressed as:

$$\gamma_{SV} = \gamma_{SL} + \gamma_{LV} \cos \theta, \quad (1)$$

where θ is the contact angle measured.

Direct measurement of the surface energy of a solid is difficult, and thus the Van Oss model [26] is adopted to calculate the surface energy for phosphate pellets and A36 steel substrates. This model considers the molecular interactions between the liquid and solid properties, resulting in the surface energy being written as:

$$\gamma = \gamma^{LW} + \gamma^{AB} \quad (2)$$

The first term γ^{LW} (Lifshitz-Van der Waals) includes all the Van der Waals forces (London, Debye and Keesom), while the term γ^{AB} is defined as:

$$\gamma^{AB} = 2(\gamma^+ \gamma^-)^{1/2}, \quad (3)$$

where γ^- and γ^+ are the electron acceptor and electron donor parameters, respectively. The expression, in Equation 4, allows direct calculation of the surface energy components of a solid.

interaction between two interfaces of this material immersed in water (w) [24]. It has two components: acid base (AB) and dispersive (LW). The expression for the interaction free energy equation is written as:

surfaces are shown in Table 1. This table also contains the values of the surface energy components (dispersive, acid and base) and also the values of the interaction free energy (hydrophobicity).

Figure 1 shows not only the evolution of the contact angle of the water but also the variation of the interaction free energy as a function of the compacting pressure. Firstly, we find that the surface of phosphate pellets has a hydrophilic character (ΔG_{iwi} is negative), we also notice that the water contact angle measured on the pellets decreases as the compacting pressure increases. We assume that for a pressure $P=90$ bar we have the highest corresponding contact angle value $\theta=28.7^\circ$ and the lowest contact angle value $\theta=17.3^\circ$ is obtained for the pressure $P = 310$ bar.

Contact angle values and surface energy components of the phosphate pellets

Phosphate pellets	Contact angle (°)			Surface Energy components (mJ/m ²)					ΔG_{iwi} (mJ/m ²)
	θ_w	θ_F	θ_D	γ^{LW}	γ^+	γ^-	γ^{AB}	γ^{Tot}	
P ₉₀	28.70	32.50	22.10	47.17	0.03	52.40	2.51	49.68	34
P ₁₁₀	25.80	31.00	22.00	47.00	0.01	54.38	1.14	48.14	34.47
P ₁₅₀	22.30	28.10	21.00	47.48	0.002	55.67	0.68	48.15	38.40
P ₂₁₀	23.00	25.30	20.10	47.78	0.02	53.00	2.06	49.84	33.60
P ₂₅₀	19.80	23.00	17.50	48.30	0.02	54.40	2.09	50.39	35.00
P ₃₁₀	17.30	20.00	13.20	49.50	0.03	55.00	2.57	52.07	34.60

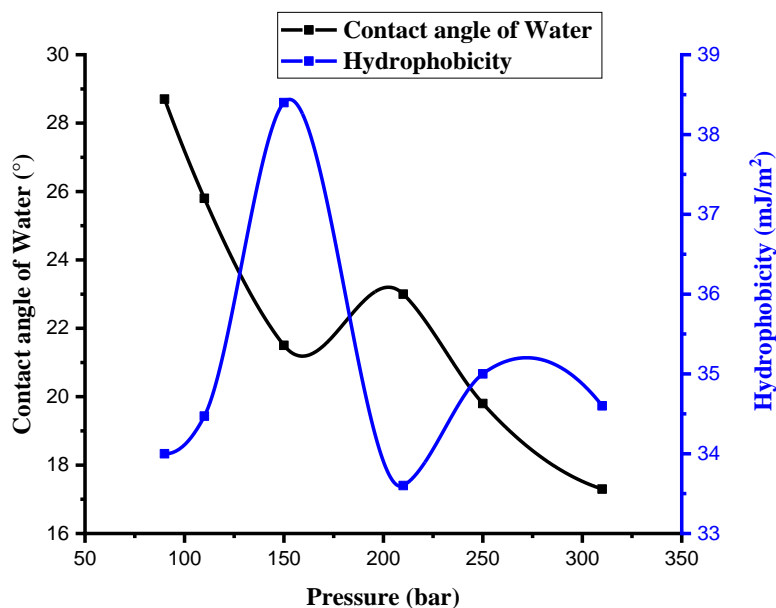


Fig. 1. Variation of the contact angle of water and hydrophobicity

We present in figure 2 the variation of the surface energy of the phosphate pellets according to the compaction pressure. The surface energy was calculated using the Van Oss modulus in order

to have a decomposition of this energy into dispersive, electron donor and electron acceptor interactions.

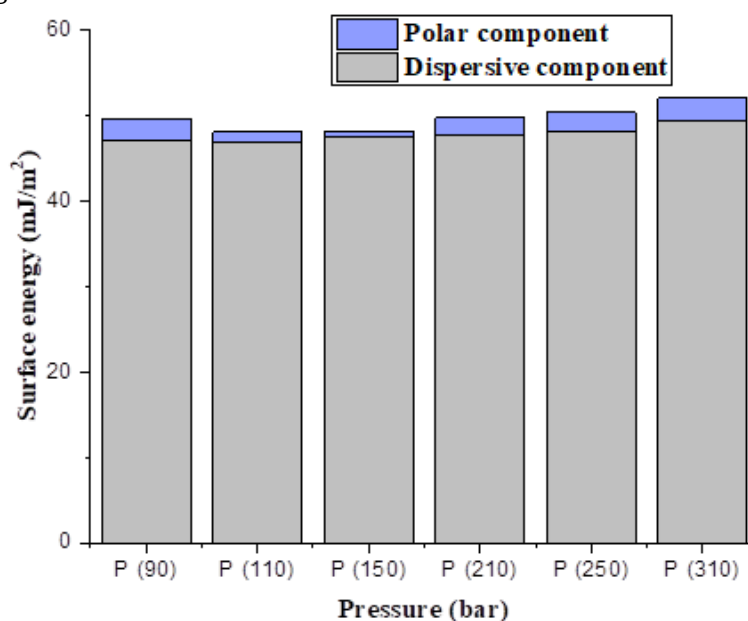


Figure 2: Surface energy components of phosphate pellets

On the one hand, the variation of the compaction pressure slightly modified the values of the surface energy of the phosphate pellets. On the other hand, we found that the phosphate surface is dominated by long-range forces, i.e. the dispersive component of the surface energy has the highest value. However, the polar component composed by the acid-base interactions has a low value. Analyzing the electron acceptor/donor character we found that the surface of the phosphate under any compacting pressure has a very important electron donor character.

Characterization of Steel A36 Surface.

Morphological characterization. Surface pre-treatment is one of the first and most important technological steps to control the processes of clogging and adhesion of materials. It is preceded by the analysis of the properties, type and

geometric structure of the material surface, as the choice of a suitable surface pre-treatment method depends on these data. Therefore, the aim is to determine the influence of topographic parameters such as the roughness of low-alloy A36 steels on the physicochemical properties. Using the metallurgical microscope (Figures 2 and 3) SOMECO 30° inclined binocular, 360° rotatable, Diopter adjustment on both eye tubes, we identified the topographic characteristics of A36 steel support according to different roughness parameters. By adjusting the surfacing conditions, we obtained surfaces with different roughnesses.

The images presented with a zoom *10 show the influence of the surface parameters that we applied on the A36 steel substrates.

The roughness was well observed according to the nature of the pre-treatment applied.

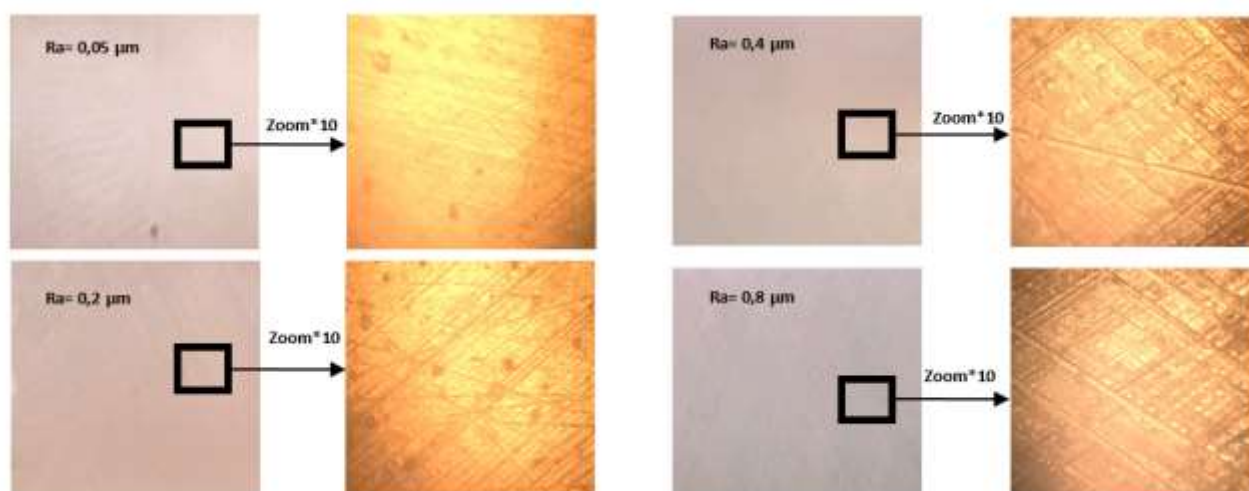


Fig. 2. Images of Steel A36 surface obtained by Honing

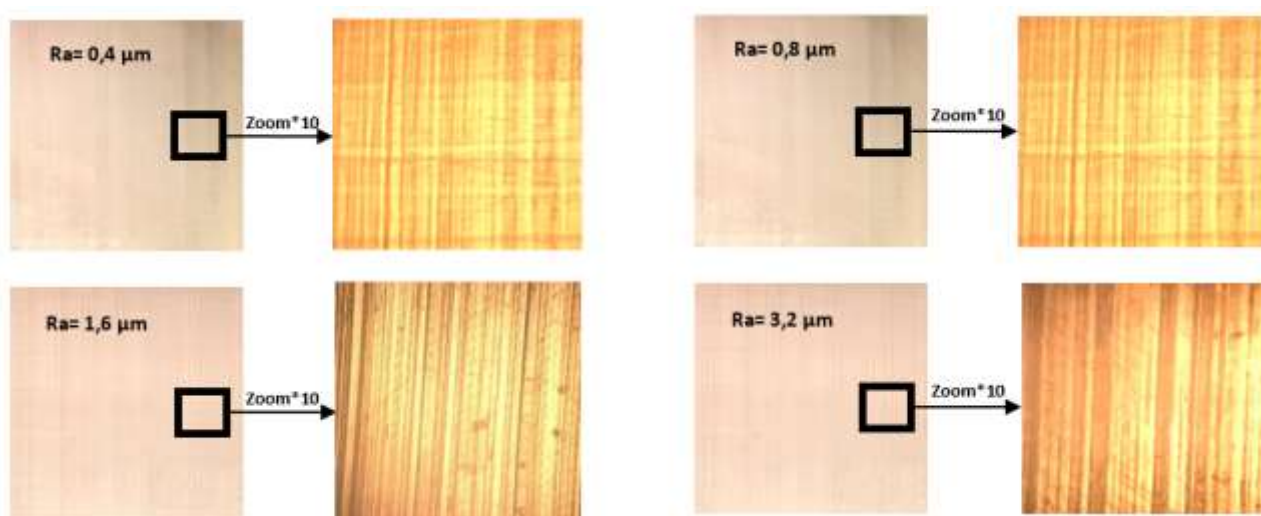


Fig. 3. Images of Steel A36 surface obtained by horizontal milling

Physicochemical characterization

The physicochemical properties of the steel surface determine the suitability of the resulting

surface layer for processes where adhesion plays an essential role. Here we are talking about adhesive properties that can be described by

different physical quantities: the contact angle and the associated wetting phenomenon, the work of adhesion and the surface energy.

Table 2

Surface energy components of A36 Steel obtained by horizontal Honing						
Roughness (μm)	Surface Energy Components (mJ/m^2)					ΔG_{iwi} (mJ/m^2)
	γ^{LW}	γ^+	γ^-	γ^{AB}	γ^{Tot}	
0.05	42.2	0.4	38.7	6.6	48.8	-3.71
0.2	40.7	0.6	36.2	9.3	50	10.45
0.4	38.8	0.2	22.8	4.8	43.6	0.97
0.8	39.2	0.1	31.1	2.4	41.6	-28.83
1.6	39	0.1	15.2	1.3	40.3	-61.66

Table 3

Surface energy components of A36 Steel obtained by horizontal milling						
Roughness (μm)	Surface Energy Components (mJ/m^2)					ΔG_{iwi} (mJ/m^2)
	γ^{LW}	γ^+	γ^-	γ^{AB}	γ^{Tot}	
0.4	33.7	0.1	10.9	1.2	34.90	-35.68
0.8	33.7	0.1	16.6	2.5	36.20	-21.05
1.6	38.9	0.2	15.2	1.3	40.20	-26.11
3.2	37.3	0.1	9.3	1.4	38.70	-42.01
6.3	30.2	0.02	12.3	1.5	31.71	-31.65

Table 2 and 3 show the development of surface energy as a function of roughness. The surface energy is calculated from the Von OSS model. After analysis of results presented in figures 4, it appears that there is a maximum value of surface energy for the roughness value for both surface treatments (honing and horizontal milling). For A36 steel substrates obtained by surface honing, we find that for a roughness of $R_a=0.2 \mu\text{m}$, we have

a maximum value of surface energy $\gamma^{Tot}=50 \text{ mJ}/\text{m}^2$ and a minimum value $\gamma^{Tot}=40,3 \text{ mJ}/\text{m}^2$ was obtained for a roughness of $R_a=1.6 \mu\text{m}$. In the case of A36 steels obtained by horizontal milling, the substrate surface of the steel has a maximum value of surface energy $\gamma^{Tot}=40.2 \text{ mJ}/\text{m}^2$ for a roughness $R_a=1.6 \mu\text{m}$ and a minimum value $\gamma^{Tot}=31.71 \text{ mJ}/\text{m}^2$ for a roughness $R_a=6.3 \mu\text{m}$.

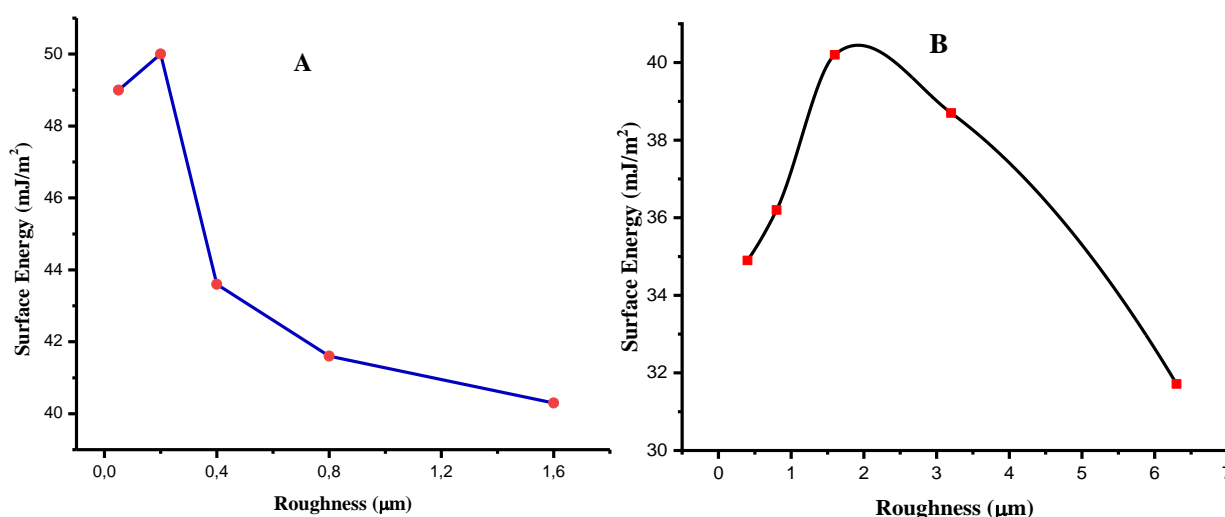


Fig. 4. Surface energy of A36 Steel Vs roughness. (A): Honing, (B): horizontal milling

Nevertheless, it can be noted that the increase in roughness has systematically decreased the surface energy values of the A36 steel. The results obtained affirm that the surface energies of A36 steel vary from high to low. We know that the molecular force of attraction between different

materials determines their adhesion. The force of attraction depends on the surface energy of the substrate. High surface energy means high molecular attraction, while low surface energy means lower attractive forces. Therefore, to decrease the clogging between phosphate and

steel substrates, we need to increase the roughness to minimize the surface energy.

The geometrical structure of the surfaces is of considerable importance from the point of view of clogging. The mechanical theory of adhesion recognizes the various factors contributing to the increase or decrease in bond strength [29-31]. These factors include surface roughness; the amount of unevenness can degrade the appearance of the adhesive. This leads us to the conclusion that the adhesive forces of the phosphates on the surface of A36 steel can be reduced if the roughness is increased.

The calculation of the interaction energy gives an approximation of the molecular interactions between two surfaces linking the hydrophobic properties to their specific roughness. We have attempted to evaluate the wetting properties of the surface of A36 steel by varying the topographic properties (roughness) in order to understand

how these properties change as a function of the free energy of interaction. From Figure 5, which shows the variation of the free energy of interaction as a function of roughness, we can see first of all that roughness affects the wetting properties and hydrophobicity. The surface of A36 steel substrates prepared by horizontal milling have a purely hydrophobic character (ΔG_{iwi} positive). The minimum value of interaction energy $\Delta G_{iwi} = -42 \text{ mJ/m}^2$ has been observed for roughness $Ra = 3.2 \text{ }\mu\text{m}$ and the maximum value of this energy $\Delta G_{iwi} = -21.05 \text{ mJ/m}^2$ has been obtained for $Ra = 0.8 \text{ }\mu\text{m}$. In addition, the surfaces of A36 steel substrates obtained by honing have a hydrophilic character at roughness levels between $0.2 \text{ }\mu\text{m}$ and $0.4 \text{ }\mu\text{m}$ and a hydrophobic character at roughness levels of $0.05 \text{ }\mu\text{m}$, $0.8 \text{ }\mu\text{m}$ and $1.6 \text{ }\mu\text{m}$. We can perceive that the substrates have a repulsive interaction.

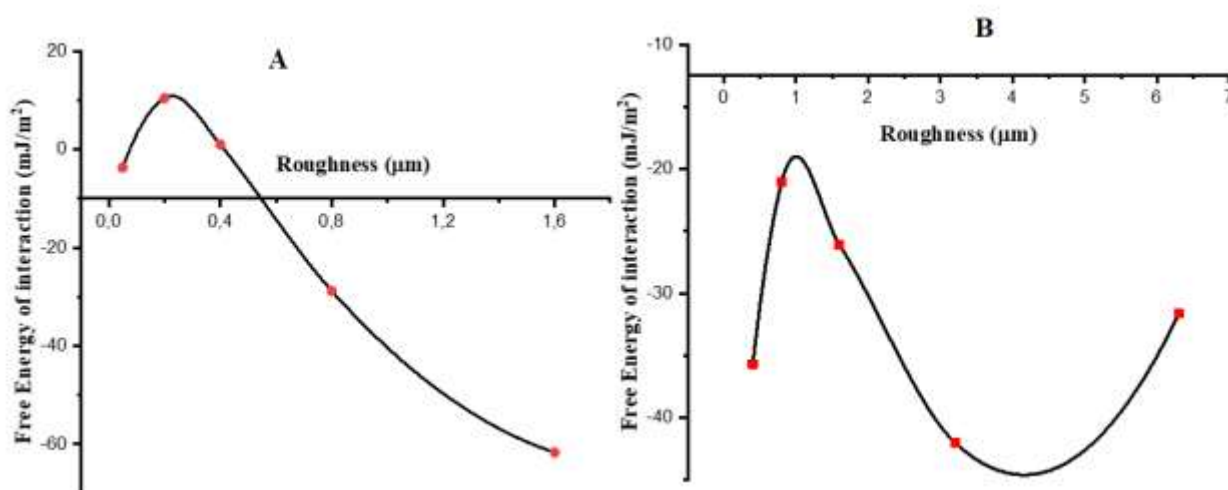


Fig. 5. Free energy of interaction of A36 Steel Vs roughness. (A): Honing, (B): horizontal milling.

Figure 6 presents a more detailed analysis of the polar and dispersive components of the surface energy of A36 steels. This analysis shows that the dispersive component represents the major part of the surface energy for the different steel substrates obtained by the two pre-treatment methods (honing and horizontal milling). For example, for a roughness of $0.2 \text{ }\mu\text{m}$ of the surface obtained by honing, the dispersive component of the surface energy represents 81% of the total surface energy and 18.6% regarding the polar component. Consequently, the interactions engaged by this type of surfaces are mainly London dispersive interactions. When the

roughness of A36 steel substrates is increased, a clear decrease in the dispersive component is observed. At the same time, the polar component of the initially low surface energy is also reduced. The London dispersive interactions, although still predominant, are therefore reduced by the increase in roughness leading to a decrease in the total surface energy. It can be concluded from this analysis that the wetting properties of A36 steel surfaces are influenced by topography and roughness. High surface roughness progressively reduces the surface energy and therefore reduces the adhesion phenomenon.

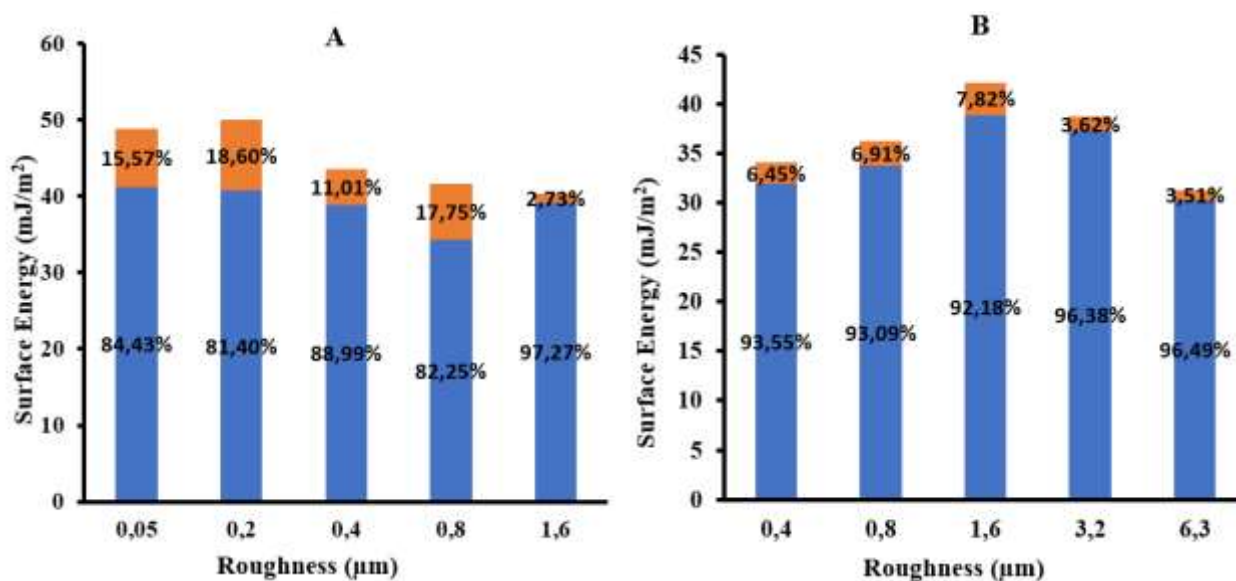


Fig. 6. Components of surface energy of A36 Steel Vs roughness. (A): Honing, (B): horizontal milling

Conclusion

In order to consider the possibility of reducing the clogging of phosphate on steels, it was essential to minimize the interactions between steels and phosphate. The challenge of this work was therefore to identify non-adhesion phenomena in order to be able to modify topographic properties such as the surface roughness of steels. First, we performed a physicochemical analysis of the phosphate pellets to extract the surface energies and also the interfacial interactions that govern them. We also established pre-treatments on A36 steels with

various roughness in order to establish a strategy oriented towards the decoupling of the surface physicochemical functionalization in order to better understand the non-adhesion of phosphate on steel supports.

The results we found showed that we can achieve a minimum energy at the interface of A36 steel by influencing the topographic parameters. Varying these parameters and the nature of the pre-treatment to obtain different roughness results in a strategy that minimizes the molecular interactions and certainly prevents the creation of chemical bonds between the phosphate and the steels.

Reference

- [1] Gooch, J. W. (2007). *Encyclopedic Dictionary of Polymers*. Springer-Verlag. <https://doi.org/10.1007/978-1-4419-6247-8>
- [2] Felder, E.; Darque-Ceretti, E. (2003). *Adhésion et Adhérence*. CNRS.
- [3] Medkour, M., Najih, Y., Bengourram, J., El Ghmari, A., Bachaoui, M., Latrache, H., Mabrouki, M. (2022). Mechanical and thermal characterization of natural phosphate: Clogging understanding (Part 1), *Materials Today: Proceedings*, 51(6), 2032–2039. <https://doi.org/10.1016/j.matpr.2021.06.261>
- [4] Baldan, A. (2004). Review. Adhesively-bonded joints and repairs in metallic alloys, polymers and composite materials: Adhesives, adhesion theories and surface pretreatment. *Journal of Material Science*, 39, 1–49. doi: [10.1023/B:jmsc.0000007726.58758.e4](https://doi.org/10.1023/B:jmsc.0000007726.58758.e4)
- [5] Meng, Y. J., Lai, J., Mo, Sh. Y., Fang, G. P., Deng, Sh. W., Wei, X. Zh., Yang, F. Y. (2023). Investigating the deterioration mechanism of adhesion between asphalt and aggregate interface under acid rain erosion, *Applied Surface Science*, 639, 158171. <https://doi.org/10.1016/j.apsusc.2023.158171>
- [6] Awaja, F., Gilbert, M., Kelly, G., Fox, B., Pigram, P. J. (2009). Adhesion of polymers. *Progress in polymer science*, 34, 948–968. <https://doi.org/10.1016/j.progpolymsci.2009.04.007>
- [7] Yin, W., Xie, Y., Yao, J., Song, N., Chen, K., Yin, X. (2023). Study on the effect of flocculation morphology on the floatability of talc flocs and the adhesion mechanism with air bubbles, *Minerals Engineering*, 203, 108317. <https://doi.org/10.1016/j.mineng.2023.108317>
- [8] Baldan, A. (2012). Adhesion phenomena in bonded joints. *International Journal of Adhesion & Adhesives*, 38, 95–116. <https://doi.org/10.1016/j.ijadhadh.2012.04.007>
- [9] Sun, J., Yamanaka, K., Zhou, Sh., Saito, H., Ichikawa, Y., Ogawa, K., Chiba, A. (2022). Adhesion mechanism of cold-sprayed Sn coatings on carbon fiber reinforced plastics, *Applied Surface Science*, 579, 151873. <https://doi.org/10.1016/j.apsusc.2021.151873>
- [10] Gerberich, W. W.; Cordill, M. J. (2006). Physics of Adhesion. *Report on Progress in Physics*, 69, 2157–2203. <https://doi.org/10.1088/0034-4885/69/7/R03>
- [11] Homma, S., Shima, M., Takano, Y., Watanabe, T., Murakami, K., Fukuda, M., Imoto, T. (2022). Hiroshi Nishikawa, Adhesion mechanism between mold resin and sputtered copper for electromagnetic wave shield packages, *Thin Solid Films*, 750, 139188. <https://doi.org/10.1016/j.tsf.2022.139188>
- [12] Stendardo, L., Gastaldo, G., Budinger, M., Pommier-Budinger, V., Tagliaro, I., Ibáñez-Ibáñez, P. F., Antonini, C. (2023). Reframing ice adhesion mechanisms on a solid surface, *Applied Surface Science*,

- 641, 158462.
<https://doi.org/10.1016/j.apsusc.2023.158462>
- [13] Bico, J., Tordeux, C., Quéré, D. (2001). Rough wetting. *Europhysics Letters*, 55, 214–220. doi:10.1209/epl/i2001-00402-x
- [14] Quéré, D. (2008). Wetting and roughness. *Annual Review of Materials Research*, 2008, 38, 71–99. <https://doi.org/10.1146/annurev.matsci.38.060407.132434>
- [15] Bico, J., Marzolin, C., Quere, D. (1999). Pearl Drops. *Europhysics Letters*, 1999, 47, 220–226. doi:10.1209/epl/i1999-00548-y
- [16] Nosonovsky, M., Bhushan, B. (2009). Superhydrophobic surfaces and emerging applications: Non-adhesion, energy, green engineering. *Curr. Opin. Colloid Interface Sci.*, 14, 270–280. <https://doi.org/10.1016/j.cocis.2009.05.004>
- [17] Lafuma, A.; Quere, D. (2003). Superhydrophobic states. *Nat. Mater.*, 2, 457–460. <https://doi.org/10.1038/nmat924>
- [18] Munoz-Bonilla, A., Bousquet, A., Ibarboure, E., Papon, E., Labrugère, C., Rodriguez Hernandez, J. (2010). Fabrication and Superhydrophobic Behavior of Fluorinated Microspheres. *Langmuir*, 2010, 26, 16775–16781. <https://doi.org/10.1021/la102686y>
- [19] Bhushan, B., Jung, Y. C. (2011). Natural and biomimetic artificial surfaces for super-hydrophobicity, self-cleaning, low adhesion, and drag reduction. *Prog. Mater. Sci.*, 2011, 56, 1–108. <https://doi.org/10.1016/j.pmatsci.2010.04.003>
- [20] Schweigert, D., Damson, B., Lüders, H., Stephan, P., Deutschmann, O. (2020). The effect of wetting characteristics, thermophysical properties, and roughness on spray-wall heat transfer in selective catalytic reduction systems. *International Journal of Heat and Mass Transfer*, 152, 119554. <https://doi.org/10.1016/j.ijheatmasstransfer.2020.11.9554>
- [21] Elyaagoubi, M., Najih, Y., Khadiri, M., Mabrouki, M. Oueriagli, A. Outzourhit, A. (2017). Electrochemically deposited Bismuth-Telluride nanowires in nanoporous alumina membranes. *Journal of Materials and Environmental Sciences*, 8, 2070–2075.
- [22] Adar, M., Najih, Y., Charafih, Y., Rahmani, K., Khaouch, Z., Mabrouki, M. (2019). Elaboration And Characterization Of ZnO Thin Films Structural And Optical Study. *Journal of Physics: Conference Series*. doi: 10.1088/1742-6596/1292/1/012009
- [23] Najih, Y. A., Charafih, M., Rahmani, Y., Khalid Khouch, Z., Jamaa, B., Nourreeddine, K., Mabrouki, M. (2019). Characterization of ZnO thin films elaborated by cathodic sputtering with different oxygen percentages: investigation of surface energy. *Journal of Physics: Conference Series*, 1292, 012015. doi: 10.1088/1742-6596/1292/1/012015
- [24] Van Oss C. J. (2006). *Interfacial Forces in Aqueous Media*, second ed, CRC Press, New York. <https://doi.org/10.1201/9781420015768>
- [25] Young, T. (1805). *An essay on the cohesion of fluids*. Phil. Trans. Soc. [Lon2d], 95, 65. <http://dx.doi.org/10.1098/rstl.1805.0005>
- [26] Van Oss, C.J., Good, R.J., Chaudhury, M.K., J. (1986). Nature of the antigen-antibody interaction: Primary and secondary bonds: Optimal conditions for association and dissociation, *Coll. Inter. Sci.*, 376, 111, 1986. [https://doi.org/10.1016/S0378-4347\(00\)80828-2](https://doi.org/10.1016/S0378-4347(00)80828-2)
- [27] Wang, X., Wei, S., Wang, X., Chang, K., Yang, H., Wang, Y. (2023). Synergetic improvements in surface hydrophobicity and wear resistance of TC4 materials via the combination of rapid heating and EtOH quenching methods, *Journal of Alloys and Compounds*, 172582. <https://doi.org/10.1016/j.jallcom.2023.172582>
- [28] Clint, J. H. (2001). Adhesion and components of solid surface energies. *Current opinion in Colloid and Interface Science*, 2001, 6, 28–33. doi: 10.1016/S1359-0294(00)00084-4
- [29] Adams, R.D. (2010). *Adhesive Bonding. Science, Technology and Applications*. UK: Wood head Publishing Limited.
- [30] Yan, C., Zhu, Y., Liu, D., Xu, H., Chen, G., Chen, M., Cai, G. (2023). Improving interfacial adhesion and mechanical properties of carbon fiber reinforced polyamide 6 composites with environment-friendly water-based sizing agent, *Composites Part B: Engineering*, 258, 110675. <https://doi.org/10.1016/j.compositesb.2023.110675>.
- [31] Brockmann, W., Geiß, P.L., Klingen, J., Schröder, B. (2009). *Adhesive Bonding. Materials, Applications and Technology*. Germany: Wiley-Vch Press, Weinheim.